THE ASTROPHYSICAL JOURNAL, 206:718–727, 1976 June 15

INFRARED SOURCES IN MOLECULAR CLOUDS*

N. Z. SCOVILLE
University of Massachusetts; and Owens Valley Radio Observatory, California Institute of Technology
AND
JOHN KWAN
State University of New York, Stony Brook; and Institute for Advanced Study
Received 1975 August 18

ABSTRACT

As a model for infrared sources in molecular regions, we calculate the radiative transfer in a dust cloud surrounding a central star. The grain temperature at each radius r is determined from radiative equilibrium in the radiation of both the star and the other circumstellar dust. In most clouds which are optically thick to the stellar photons, heating by the dust reradiation is dominant. However, even with moderate opacity ($\tau_{100\,\mu} \lesssim 1$), the temperature distribution with radius stays qualitatively similar to that of an optically thin envelope. Different portions of the infrared spectrum may help pinpoint the parameters characterizing the source. We find that (1) the spatial variation of the flux at $\lambda \geq 350\,\mu$ provides an excellent measure of the dust density distribution, (2) the falloff in intensity longward of the spectral peak is always slower than $\lambda^{-(2+n)}$ for an λ^{-n} emissivity law, (3) the optical depth at the peak will always be less than or about unity, (4) a power-law form for S_ν in the near-infrared quite generally indicates that the emission is optically thin, and (5) an exponential decrease in S_ν in the near-infrared implies either that $\tau \approx 1$ at the peak or that there is a deficiency of grains at small r.

Viewing the observational data for the Kleinmann-Low nebula in light of the models, we infer that the dust density distribution is $n_d \propto r^{-1.5}$, the long wavelength emissivity between 30 μ and 1 mm varies approximately as $\lambda^{-1.5}$, and $\tau_{70\,\mu} \approx 1$.

Subject headings: infrared: sources — nebulae: general — radiative transfer

I. INTRODUCTION

Powerful infrared sources, sometimes exceeding $10^5\,L_\odot$, have recently been discovered deep within the vast clouds of molecular gas distributed through the galactic plane. But though the ultimate source of energy is a compact object of stellar size emitting at optical wavelengths, the observed long wavelength radiation ($\lambda \gtrsim 20\,\mu$) is seen from an extended source typically 1 pc in diameter. This has led to the understanding that an extensive cloud of dust optically thick to the primary photons envelops the central star. The spectrum of radiation escaping from the cloud is that of the radiatively heated dust; it will depend not only on the properties of the central star (mostly its luminosity), but even more importantly on the dust density distribution and its emissive properties.

The gas within the same dust clouds has been extensively studied, its distribution mapped and physical conditions determined, by the molecular emission lines of CO, CS, and HCN at millimeter wavelengths. A study of the dust envelope will aid us not only in learning the emissive properties of the grains but also, together with the molecular observations, in understanding the cloud structure and the relationship between the dust and the gas in these dense interstellar clouds. A detailed analysis is warranted as the density of the gas, the dust-to-gas ratio, and the thermal coupling between the gas and the dust all play a role in determining the observed infrared and molecular properties.

Here we will examine how the radiative heating in an *optically thick* dust cloud may depend on the properties of the dust, its distribution, and the central luminous source. To this end, we have calculated the falloff of the grain temperature with radius in the cloud such that each grain is in radiative equilibrium. The spectra and angular distribution of the emitted infrared radiation are obtained from this temperature distribution and compared with observations to delimit the free parameters and to discriminate between various alternate models.

The equations governing the radiative equilibrium and our adopted model for the dust cloud are presented in the next two sections. Following these, several general results of the *continuum* radiative transfer are presented, and the infrared source at the Orion molecular cloud, the Kleinmann-Low nebula, is discussed in detail. In a second paper (Kwan and Scoville 1976) we treat the formation of *narrow spectral features* such as the silicate and ice features in the near-infrared.

* Sponsored in part by NSF grants GP-40768X (J. K.), GP-30400-X5 (N. S.), MPS 73-04949 A01 (N. S.).

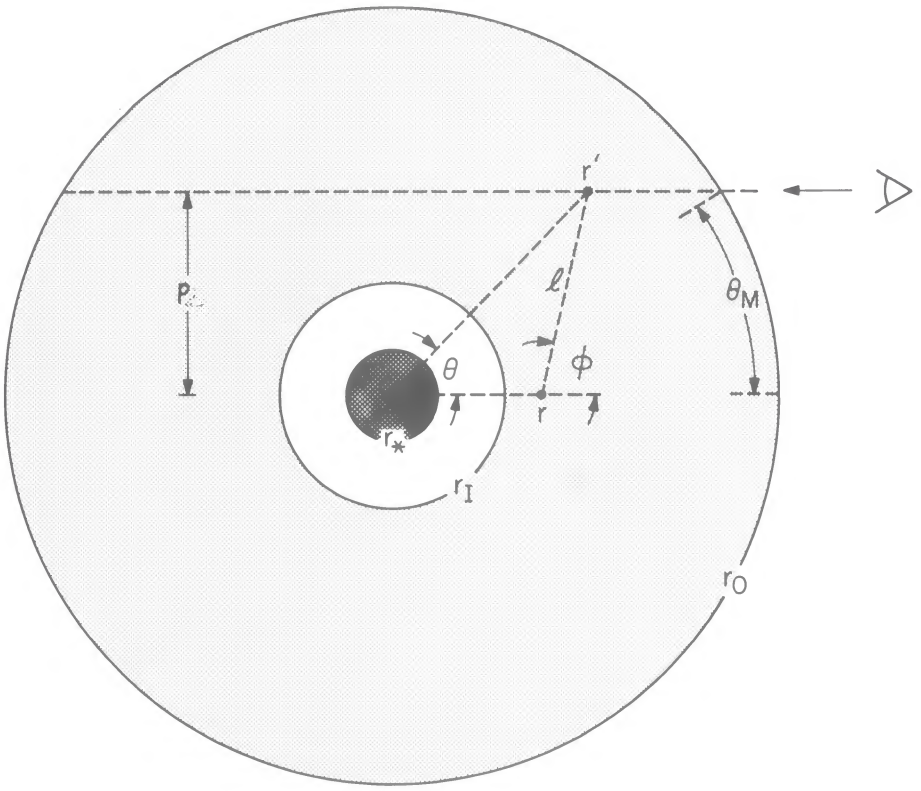

FIG. 1.—A geometrical picture of the cloud showing the coordinates employed in eqs. (1) through (6). The cloud is a spherical shell between radii r_I and r_0 centered on the star.

II. RADIATIVE EQUILIBRIUM OF DUST

We consider a spherical cloud of dust and gas surrounding a central luminous blackbody. The central source is characterized by a temperature T_* and radius r_*, and the dust cloud extends from an inner radius r_I to an outer radius r_0 (Fig. 1).

For a grain of radius a located at a distance r from the central source, the rate of energy gain from absorption of the stellar radiation is

$$W_{\text{star}}{}^{+} = \int_0^\infty d\nu \pi B_\nu(T_*) \frac{r_*{}^2}{r^2} \pi a^2 \epsilon_\nu \times \left\{ \exp\left[-\int_{r_I}^{r} n_d(r') \pi a^2 \epsilon_\nu dr' \right] \right\}, \quad (1)$$

where $B_\nu(T)$ is the Planck intensity, $2h\nu^3 c^{-2}/(e^{h\nu/kT} - 1)$, $n_d(r)$ the number density of grains, and ϵ_ν the dust emissivity.

Since we are interested in the infrared spectrum at $\lambda > 5\,\mu$, we neglect the effect of scattering by the grains and assume that the grains are isotropic. The rate of energy gain from absorption of radiation emitted by other grains is

$$W_{\text{dust}}{}^{+} = \int_{r_I}^{r_0} n_d(r')(r')^2 dr' \int_0^\pi \beta(r', \theta) 2\pi \sin\theta d\theta, \quad (2)$$

where θ is the polar angle in a coordinate system (Fig. 1) with the Z axis in the direction of the grain at radius r. The variable $\beta(r', \theta)$ represents the rate of energy gain from a single dust grain at (r', θ) and is given by

$$\beta(r', \theta) = \int_0^\infty d\nu \pi B_\nu[T_d(r')] \frac{a^2}{l^2} \pi a^2 \epsilon_\nu \times \left[\exp\left(-\int_0^l n_d \pi a^2 \epsilon_\nu dl' \right) \right], \quad (3)$$

where l is the chord length between (r', θ) and $(r, 0)$.

The equilibrium temperature of the grain at radius r, $T_d(r)$, is obtained by balancing the sum of the two rates of heat gain given above against its rate of heat loss. The latter rate is

$$W^{-} = \int_0^\infty d\nu \pi B_\nu[T_d(r)] 4\pi a^2 \epsilon_\nu . \quad (4)$$

The spatial integrals were evaluated numerically by dividing the cloud into 10 to 30 concentric shells, with logarithmically increasing radii spanning r_i to r_0, and dividing the range of θ ($0 \leq \theta \leq \pi$) into 10 sectors. Integrals over frequency were done by first locating the frequency at which the integrand was maximum, and then evaluating the integral from a quadrature of 10 neighboring frequency points. The solution was

found by resubstitution (an initial guess of the temperature distribution was obtained by neglecting the heat input from surrounding dust grains) and was judged satisfactory if the temperatures at all radii changed by less than 0.5 percent. To be assured that a converged solution had been found, several additional iterations were done using Newton's method to give formal errors less than 0.001 percent and a rapid rate of convergence. The errors which remain at this point result from the practical necessity of dividing the cloud into a finite number of shells and assuming that the temperature is constant in each shell. Thus, as an additional check of the accuracy, the power emergent from the cloud was required to be within 10 percent of the luminosity of the central source.

To provide a most straightforward comparison with observations, we calculate the flux density S_ν observed, at a distance d from the cloud, within a circular aperture of radius p about the center (see Fig. 1):

$$S_\nu(p) = \frac{1}{d^2}\int_0^p I_\nu(p')2\pi p'dp' , \tag{5}$$

where

$$I_\nu(p') = p'\int_{\theta_m}^{\pi-\theta_m} d\theta \csc^2(\theta)\pi B_\nu[T_d(r)]a^2\epsilon_\nu n_d(r) \times \left\{\exp\left[-\int_{\theta_m}^{\theta} n_d(r)\pi a^2\epsilon_\nu p' \csc^2(\theta')d\theta'\right]\right\}. \tag{6}$$

The angle θ is related to r by $\theta = \arcsin(p/r)$, and $\theta_m = \arcsin(p/r_0)$.

III. PARAMETERS OF THE MODEL

The principal parameters entering the model are the luminosity, the inner and outer cloud radii, the dust density distribution with radius, and the dust emissivity. The luminosity is usually known from observations and is $10^5 L_\odot$ for the Kleinmann-Low nebula (Werner *et al.* 1975). The inner and outer radii are unknown, but the calculated results are not sensitive to their exact values. Unless the cloud is a thin shell, the dominant emergent radiation will originate from radii much farther away from the inner boundary and will not depend crucially on the location of the latter. The precise outer radius is also not critical to the results. Outer layers are never important to the heating of layers more interior, and therefore the calculated spectrum will remain unchanged unless the outer layers contribute a large opacity at far-infrared wavelengths. Even then, because the size of the cloud always enters the model calculations together with the density, any uncertainty in the extent of the cloud, in the absence of detailed far-infrared maps, can be replaced by a corresponding uncertainty in the overall density. More important then is the total opacity through the cloud at a suitable wavelength. A good estimate of this parameter can actually be obtained from the observed spectrum. We will show in the next section that at the wavelength where the spectrum peaks the opacity through the cloud is generally near or less than unity.

The density distribution and emissivity law of the grains constitute the most uncertain entities of the model. They are also the most crucial parameters in influencing the calculated spectrum, mainly through controlling the radial and frequency dependence of the opacity. Since these two distributions are *a priori* unknown, it would not be difficult to arbitrarily vary them in order to perfectly match the more limited observations. It is suspected, however, that such a process could be done in several ways and a unique solution will not be found. To avoid such indiscriminate calculations, we have adopted only simple forms for the density and emissivity distributions; they are a power-law dependence in the density,

$$n_d(r) = n_d(r_i)\left(\frac{r_i}{r}\right)^\alpha , \quad \alpha \geq 0 , \tag{7}$$

and a three-part power law in the emissivity,

$$\begin{aligned} \epsilon_\nu &= 1 , && \nu > \nu_1(\equiv c/\lambda_1) , \\ &= \nu/\nu_1 , && \nu_1 \geq \nu \geq \nu_2(\equiv c/\lambda_2) , \\ &= \nu^2/\nu_1\nu_2 , && \nu_2 > \nu . \end{aligned} \tag{8}$$

We shall neglect the scattering of radiation by grains. At far-infrared wavelengths the mean free path for pure scattering is longer than that for absorption, and the approximation is good. At near-infrared wavelengths the scattering length might be shorter, but as long as the opacity for absorption at those wavelengths is greater than five, the neglect of pure scattering will not seriously affect the temperature and spectral distributions. Knacke and Thomson (1973) have obtained emissivity measurements of silicate particles for $1\,\mu < \lambda < 1$ mm. At $\lambda < 30\,\mu$, the silicates possess strong resonances (notably at $\lambda = 10\,\mu$ and $20\,\mu$), while at much longer wavelengths the absorption efficiency falls as λ^{-2}. Unfortunately, though many astronomical infrared sources do show the silicate features at 10 and $20\,\mu$, it is unknown if this component in interstellar grain materials gives the dominant opacity at any other wavelength.

The power-law index α in the density distribution is taken between 0 and 2, λ_1 is usually $0.1\,\mu$, and λ_2 between $20\,\mu$ and $100\,\mu$. The total opacity through the cloud is specified at $100\,\mu$ through the parameter $\tau_{100\,\mu}$.

Ten models differing in density distribution, optical depth $\tau_{100\,\mu}$, and emissivity law illustrate the effects of changes in each parameter. A summary of the results for four models relevant to our discussion of the Orion source in § V is provided in Table 1, including half-power sizes at various wavelengths, the wavelength of peak S_ν as measured in different aperture sizes, the dust temperature, and its radial gradient at $r = 2 \times 10^{17}$ cm (corresponding to 30″ at 500 pc). For some models spectra and temperature profiles are also shown in Figures 2 through 4.

IV. GENERAL PROPERTIES OF THE RADIATIVE TRANSFER

In a crude way we may understand the temperature distribution and the emergent spectrum from a dust cloud without resort to numerical calculations.

TABLE 1

MODELS FOR KL NEBULA*

PARAMETERS		HALF-POWER SIZE (arcsec)†				PEAK‡				
$\tau_{100\,\mu}$	λ_2 (μ)	$\psi_{10\,\mu}$	$\psi_{20\,\mu}$	$\psi_{50\,\mu}$	$\psi_{100\,\mu}$	5″	1′ (μ)	7′	T_d (K)§	$d \ln T_d / d \ln r$
I. 0.1....	100	1.0	3.5	30	140	15	46	110	71	−0.43
II. 0.5....	100	0.8	2.9	25	105	25	64	120	63	−0.43
III. 2.5....	100	0.8	3.3	12	52	66	100	135	47	−0.43
IV. 0.5....	30	1.5	6.0	30	135	45	65	100	69	−0.41

* For all models $r_1 = 10^{15}$ cm, $r_0 = 2$ pc, $T_* = 3600$ K, $L_* = 10^5\,L_\odot$, $\lambda_1 = 0.1\,\mu$, and $n_d \propto r^{-1}$.

†The half-power sizes are defined as the diameter of a circular diaphragm which contains 50% of the total flux density escaping the cloud at the given wavelength for an assumed distance of 500 pc.

‡ The wavelengths of maximum flux density λ_{peak} were calculated for 5″, 1′, and 7′ apertures centered on the star.

§ At $r = 2 \times 10^{17}$ cm.

a) Temperature Distribution

The total luminosity of an infrared source places an upper limit on the dust temperature at each spatial point. This upper limit is calculated by assuming no intervening opacity between the central source and the grain in consideration; that is, by balancing the heat gain from absorption of the full stellar radiation (eq. [1]) against the radiative heat loss (eq. [3]). This calculation has a simple analytic solution if the following approximations are made: first, that the central source radiates primarily at a wavelength where the dust emissivity is near unity ($\lambda \leq 1\,\mu$), and, second, that the emissivity at far-infrared wavelengths has the form $f(50\,\mu/\lambda)^n$. The emissivity law has been approximated by a power law about 50 μ, because most luminous infrared sources peak near that wavelength. The value of the emissivity at 50 μ, f, is taken to be an additional parameter in order not to extrapolate on the frequency dependence of the emissivity at wavelengths much shorter than 50 μ. With these simplifications, the upper bound on the temperature distribution is

$$T_d(r) = 49^\circ f^{-1/5}\left(\frac{2\times 10^{17}\ \mathrm{cm}}{r}\right)^{2/5}\left(\frac{L_*}{10^5\,L_\odot}\right)^{1/5}, \quad n=1,$$

$$= 51^\circ f^{-1/6}\left(\frac{2\times 10^{17}\ \mathrm{cm}}{r}\right)^{1/3}\left(\frac{L_*}{10^5\,L_\odot}\right)^{1/6}, \quad n=2. \tag{9}$$

The normalizations, $L_* = 10^5\,L_\odot$, $r = 2 \times 10^{17}$ cm, are so chosen as to model the Kleinmann-Low nebula (KL). Two conclusions can be drawn from the above solution. Observation of the CO, $J = 1 \rightarrow 0$ line shows a brightness temperature of 70 K over a 1′ beam, a result indicating that the gas temperature is about 70 K at a radius of 2×10^{17} cm. We expect the grains to be hotter than the gas in order that they be responsible for heating the latter (cf. § IV*f*). From equation (9), this condition imposes that the emissivity at

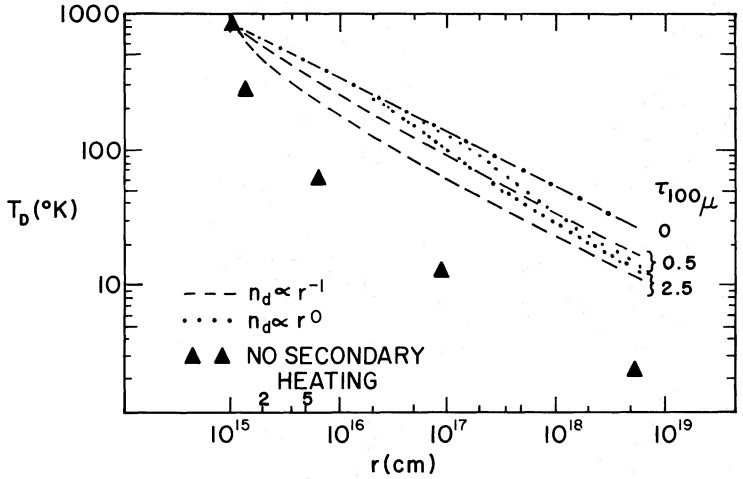

FIG. 2.—The decrease in dust temperature away from the central star for models with density varying as r^{-1} (*dashed curves*) and r^0 (*dotted curves*) for optical depth $\tau_{100\,\mu} = 0$, 0.5, and 2.5.

The importance of heating by dust reradiation (eq. [2]) may be judged from the triangles which are the temperatures calculated with only the heating from the attenuated starlight included, using the model with $n_d \propto r^{-1}$ and $\tau_{100\,\mu} = 2.5$.

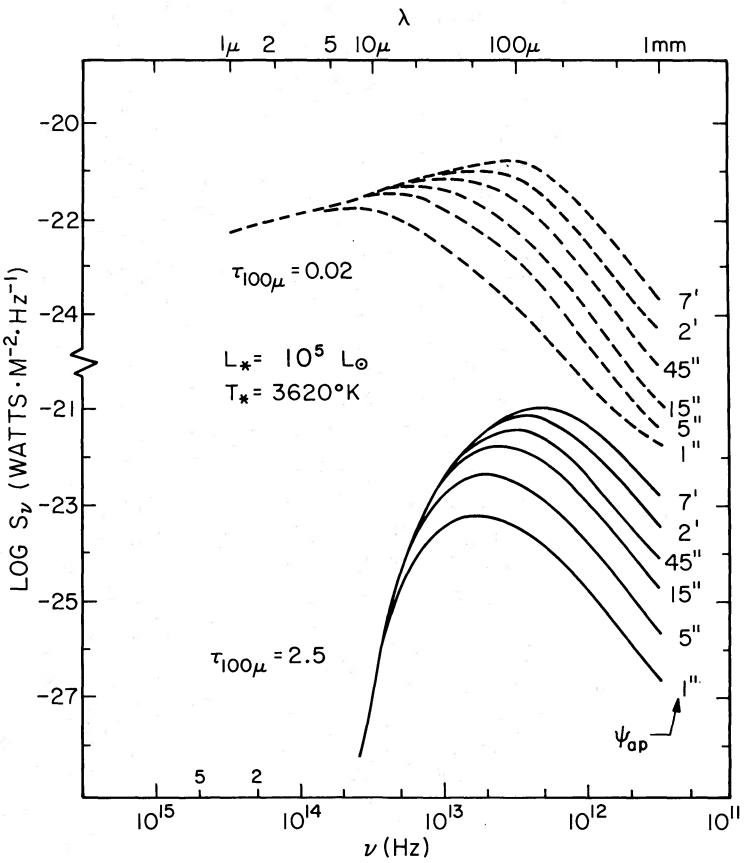

FIG. 3.—Spectra of optically thin and thick models with $n_d \propto r^{-1}$ and observed with various apertures. The aperture sizes are for a distance of 500 pc. Note that the optically thin source has a power-law spectrum in the near-infrared and that the wavelength of peak emission is redshifted for larger apertures.

50 μ, f, be less than 0.09 and 0.07 for $n = 1$ and 2, respectively. Second, the analytic solution indicates a radial dependence in the temperature distribution which is insensitive to the emissivity law, the ratio of the two distributions for $n = 1$ and 2 being proportioned to $r^{1/15}$. The temperature at each position, on the other hand, depends quite strongly on f. If the same power-law dependence of the emissivity holds at short wavelengths, so that f equals 0.02 and $(0.02)^2$ for $n = 1$ and 2, respectively (assuming an emissivity of unity at 1 μ), the two temperature distributions given by equation (9) would differ by a factor of 1.7 at $r = 2 \times 10^{17}$ cm, being 108 K and 180 K for $n = 1$ and 2, respectively.

While the above determination of temperature is correct only for a dust cloud optically thin at all wavelengths, it can provide a fair approximation (to 50%) even when the opacities at near-infrared wavelengths are substantial ($\tau_{2\mu}$ up to 20). In Figure 2, we compare this upper limit on the temperature distribution (using the three-part power law of eq. [8] for the emissivity, with $\lambda_1 = 0.1$ μ and $\lambda_2 = 100$ μ) with the correct temperature distribution from numerical calculations which take into account the opacity of intervening grains and their reradiation. The dashed curves refer to calculations made assuming a density decreasing with radius ($\alpha = 1$), and the dotted curves to calculations made using a constant density distribution. For both distributions the outer radius of the dust cloud was taken to be 2 pc and the total opacity through the cloud at 100 μ specified as 0.5 and 2.5.

The numerical models follow the analytic solution closely out to where interior dust becomes opaque at the peak of stellar emission, at which point the exact T_d falls below equation (9). Figure 2 also illustrates the importance of heating due to reradiation from hot dust. The triangles in that figure give the temperature distribution that would result if only the stellar radiation, attenuated by intervening dust, were included in the heating. In the numerical examples, the temperature of the star was taken to be 3600 K. In clouds optically thick to the stellar radiation, the particular stellar temperature has little effect on the dust temperature distribution, as the diffusing radiation quickly loses memory of T_* due to the low one-fifth order dependence of T_d upon the wavelength of the radiation incident on the grain.

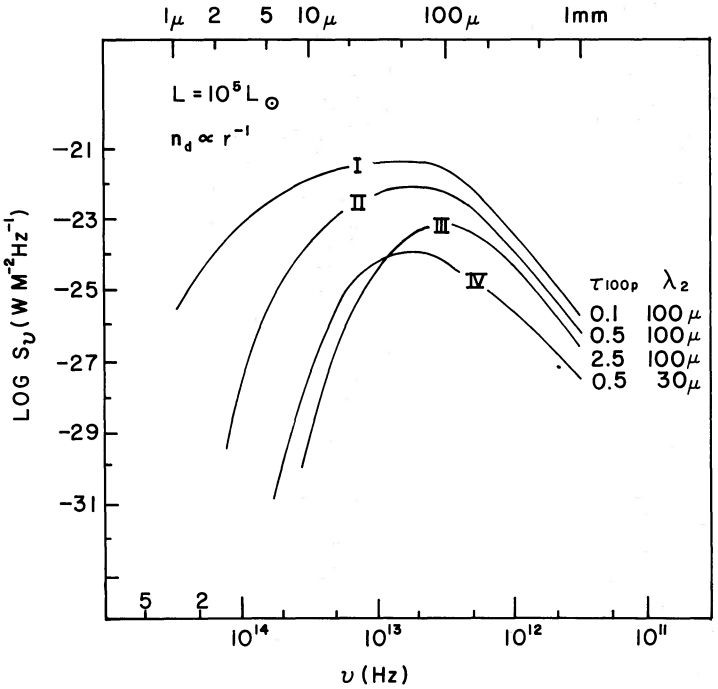

FIG. 4.—Spectra of models relevant to the discussion of the Kleinmann-Low nebula (Table 1). For the first three models the total optical depth at 100 μ, $\tau_{100\,\mu}$, takes the values 0.1, 0.5, and 2.5 while the emissivity law ϵ_λ is held constant ($\epsilon_\lambda \propto \lambda^{-1}$ for $\lambda < 100\,\mu$ and $\epsilon_\lambda \propto \lambda^{-2}$ for $\lambda > 100\,\mu$). In the fourth spectrum, the emissivity law is changed ($\epsilon_\lambda \propto \lambda^{-1}$ for $\lambda < 30\,\mu$, and $\epsilon_\lambda \propto \lambda^{-2}$ for $\lambda > 30\,\mu$) and $\tau_{100\,\mu}$ is set at 0.5. For all models $L_* = 10^5\,L_\odot$, $n_d \propto r^{-1}$, and the flux density in a 1′ diameter aperture, S_ν, is calculated for a distance of 500 pc. The successive spectra have been shifted down by a factor of 10 for the display.

b) *Emission Peak*

It is useful to recognize that the opacity cannot be much greater than unity at the *peak* of an observed spectrum. We demonstrate this as follows. The intensity observed from a particular grain at a depth τ_ν along the line-of-sight is proportional to

$$B_\nu(T_d)\epsilon_\nu \exp(-\tau_\nu)\,.$$

As an example let $\epsilon_\nu \propto \nu$ and $\tau_\nu = \nu/\nu_0$ so that at ν_0 the opacity is unity. Then the intensity from the grain peaks at $\nu_m \approx 4\nu_0/(1 + h\nu_0/kT_d)$ and at ν_m the opacity is $\tau_{\nu_m} \lesssim 4 - h\nu_m/kT_d$. In most observed infrared sources, the wavelength at the spectral peak and the corresponding color temperature are such that $h\nu_m/kT$ is $2 \rightarrow 4$, and the approximation that the opacity through the cloud is less than or about unity at the peak is a condition which is often approached.

One expects the spectral peak to shift to a longer wavelength as the aperture size is increased, since a larger region with lower dust temperatures will be covered. Conversely, when the aperture size (centered on the source) is decreased, the peak will shift to higher frequency. This blueshifting will continue only as long as the source continues to be optically thin at the successively shorter wavelengths. Once the source is optically thick at the peak wavelength as observed with a given aperture, the discussion above indicates that no further shift will occur when an even smaller aperture is employed. Observations at differing aperture sizes therefore can provide a straightforward and reliable means of discriminating optically thick and thin clouds.

These general properties are illustrated in Figure 3 where the calculated spectra of two clouds differing only in their total opacity are presented for a series of aperture sizes. The parameters of the models are $L_* = 10^5\,L_\odot$, $\alpha = +1$, $\lambda_2 = 100\,\mu$, $r_0 = 2$ pc, and $\tau_{100\,\mu} = 0.02$ and 2.5. The aperture sizes are specified for a distance of 500 pc.

Parenthetically, we note that if it is true that the wavelength of peak emission tends to be longer when the source is observed with a bigger aperture (i.e., less spatial resolution), then this shift will also be noticeable in comparing spectra of similar sources at different distances. The source farther away will have its peak redshifted relative to the closer one. For this reason it could be misleading to conclude that the source Sgr B2 at a distance of 10 kpc is necessarily of extraordinarily high opacity *just* because its peak is very red ($\lambda \gtrsim 100\,\mu$).

c) *Near-Infrared*

In general, the lengthy procedure of obtaining and comparing spectra with several different apertures will not be required in order to crudely classify thin and thick sources. Instead, the shape of the near-infrared spectrum, whether it is power law or exponential, may

be used as a cue. All models having density constant or increasing inward contain enough hot grains near the star that the short wavelength fluxes in optically thin clouds are power law in form. Thus optically thin clouds with density varying as r^0, r^{-1}, and r^{-2} have near-infrared spectra S_ν of the form ν^{-3}, $\nu^{-0.8}$, and $\nu^{1.4}$ observed with a large beam taking in all the source at each frequency (assuming $\epsilon_\nu \propto \nu$). The only means found to give the exponential decrease in S_ν observed in many extended sources is through absorption in the near-infrared by outer layers or through a *decreasing* dust density at small radii so that there is a deficiency of hot grains.

d) Far-Infrared

The spectral region longward of the peak can yield information about the emissivity law at those wavelengths and the dust density distribution. To first approximation, the flux density in that spectral range decreases with decreasing frequency as $S_\nu \propto \nu^{2+n}$, where the factor ν^2 comes from the Rayleigh-Jeans dependence of the blackbody intensity on frequency, and the factor ν^n from the assumed emissivity. The $2 + n$ power in frequency is never fully realized in actual observed spectra for the following two reasons. First, the above result assumes that the emission over that spectral range is not absorbed by intervening grains. However, even though the opacities are small, the relatively higher opacity at a shorter wavelength always decreases the observed intensity at the shorter wavelength. Second, and more importantly, the dust temperature decreases with radius, and at low temperatures the blackbody emission at the higher frequency might not lie on the Rayleigh-Jeans portion. For example, at a dust temperature of 50 K, the ratio of the blackbody intensity at 200 μ and 1 mm is 12.5 rather than 25. The model calculation presented in Figure 3 demonstrates this effect. For the spectrum observed over a 1′ beam, the intensity increases with frequency over the range 200 μ–1 mm as $S_\nu \propto \nu^{3.3}$, instead of ν^4. With a constant density distribution where the cooler dust contribute a larger amount of the emission at long wavelengths, the difference is slightly larger, $S_\nu \propto \nu^{3.1}$. Thus, if an observed spectrum is fitted by the approximation $S_\nu \propto \nu^{2+n}$ longward of the peak, the value of n so obtained is a lower bound and the actual value could easily be 0.5 higher.

Spatial maps of the emission on the Rayleigh-Jeans tail at $\lambda = 350\ \mu$ or 1 mm provide a good indication of the density distribution within a source. The flux density at these wavelengths is proportional to the volume integral of the product of the grain temperature and density contained in the observing aperture. Since the temperature contains only a weak spatial dependence, $T_d \propto r^{-2/5}$, major variations in the long wavelength flux density must be due to changes in the mass distribution of grains. For a cloud of constant density, the long wavelength intensity I_ν given by equation (6) varies with impact parameter (see Fig. 1) only as $\sim p^{-0.1}$. Stronger spatial variation is observed near the centers of several of the regions mapped at 350 μ and 1 mm by Righini *et al.* (1975) and Harvey *et al.* (1974). In sources like the Orion Nebula or Sgr B2 densities must sharply rise within the core of the source. Such a sure statement regarding the density distribution cannot be made from shorter wavelength measurements where the source is likely to be optically thick and the fluxes sensitive to the grain temperature distribution. High angular resolution observations at $\lambda \geq 350\ \mu$ are therefore most important for determining the density distributions.

e) "Silicate" Features

In addition to the infrared continuum spectrum we have modeled the near-infrared ice and silicate resonance features at 3.1 μ and 10 μ (and 20 μ). Many sources show these features in absorption, especially those objects for which there is other basis to infer large column densities of foreground dust. Since often the depth of the 10 μ silicate absorption is taken as an independent measure of dust column density, we thought it worthwhile to see how reliable this might be. In optically thick sources ($\tau_{10\,\mu} > 1$) having a falloff of grain density with radius ($n_d \propto r^{-1}$ or r^{-2}), we find that the presence of a temperature gradient in the source leads quite naturally to substantially less emission from the source at 10 μ than at neighboring frequencies. Thus many of the objects where the 10 μ absorption is seen may not require additional foreground dust if the absorption is an "atmospheric" effect, intrinsic to the source spectrum. (The 10 μ feature will be in emission only if the source is optically thin.) Our results for these discrete spectral features are presented in a second paper (Kwan and Scoville 1976).

f) Relationship to Molecular Gas

Thermal coupling between the radiatively heated dust grains and ambient molecular gas (H_2) has been investigated by Goldreich and Kwan (1973). They indicated that the gas will approach thermal equilibrium with the dust ($T_K \rightarrow T_d$) via collisions of H_2 with grains (at $n_{H_2} > 10^4\ \mathrm{cm}^{-3}$). Unfortunately, even at $n_{H_2} = 10^4\ \mathrm{cm}^{-3}$ the collisional rate is sufficient to give only $T_K \approx T_d/2$. Observational evidence, however, suggests that the coupling may be stronger. Over large regions in the galactic center the brightness temperature of $J = 1 \rightarrow 0$ CO emission (commonly interpreted as a measure of T_K) is within observational uncertainties equal to the brightness temperature of 100 μ infrared emission (Scoville, Solomon, and Jefferts 1974).

A more rapid transfer of energy from dust to gas may exist through absorption of dust radiation in the rotational transitions of water molecules followed by collisional de-excitation by H_2. With numerical calculations of the H_2O excitation equilibrium similar to Kwan and Thuan (1974), we have verified that this process is generally faster than direct H_2 collisions with grains. For the radiation field in a dust cloud characterized by $T_d = 45$ K and $\tau_{100\,\mu} = 1$ and a density $n_{H_2} = 5 \times 10^3\ \mathrm{cm}^{-3}$, about 10 percent of the

H_2O molecules will be excited into the 2_{12} level at an energy corresponding to 80 K (a $\lambda = 180\ \mu$ transition) above the ground state. From this level efficient heating may occur by absorption of a 75 μ photon (transition from 2_{12} up to 3_{21}) and the subsequent collisional de-excitation.[1] For a *minimal* abundance ratio $H_2O/H_2 = 3 \times 10^{-6}$ the rate of heating is 10^{-23} ergs s^{-1} cm^{-3} at $T_K = 30$ K. (For comparison the cooling rate by CO molecules at an abundance $10^{-4}\ n_{H_2}$ will be an order of magnitude less.) When T_K is raised to 40 K, we find that the situation is reversed and the H_2O cools the H_2. For these *illustrative* parameters the kinetic temperature will be 35 K in thermal equilibrium when the H_2O neither heats nor cools the H_2.

We therefore expect that even in clouds of moderate density with $n_{H_2} = 10^4$ cm^{-3} the gas temperature will be closely coupled to the dust temperature. This will be true unless there is an additional heating input to the gas serving to raise T_K above T_d.

V. KLEINMANN-LOW NEBULA

As an application of the dust model, and an illustration of its general properties, the Kleinmann-Low nebula, with its large amount of observational data, is chosen to be modeled. Observed fluxes at various wavelengths in this nebula and also at the Becklin-Neugebauer object (BN) are shown in Figure 5. Flux densities at $\lambda > 20\ \mu$ were obtained with 1′ resolution; those for $\lambda < 20\ \mu$ are from integrations of higher resolution maps over a 1′ aperture. Use of low resolution 10 μ and 20 μ observations at KL might be an error, since much of the low surface-brightness emission picked up at low resolution could be due to the nearby H II region.

a) Selection of the Model Parameters

Based on the general properties of the dust radiative transfer (cf. § IV), we can already limit the choice of the various parameters that enter into modeling KL.

From the spectral observations longward of the 70 μ peak, both the dust emissivity law and the density gradient in the outer portion of KL may be inferred. The best evidence for a rapid decrease in the density outside $r = 10^{17}$ cm is provided by maps at $\lambda = 1$ mm, which show a decrease to half-intensity only 1′ from the center (Harvey *et al.* 1973). Unmistakably, this observation implies a density falloff, since an optically thin, Rayleigh-Jeans approximation for the 1 mm emission is valid and the dust temperature is slowly changing with radius. Models with density varying as r^0, r^{-1}, and r^{-2} give intensity $I_\nu(p)$ (eq. [6]) dependent on p as $p^{-0.05}$, $p^{-0.6}$, and $p^{-1.5}$ in the range $p = 10^{16}$ to 10^{18} cm. The best match to the observed intensity gradient is for a density decrease slightly steeper than r^{-1}. In the model calculations we shall just use a r^{-1} distribution.

[1] The other transitions in order of decreasing importance are $2_{21} \rightarrow 3_{30}$ ($\lambda = 66\ \mu$), $3_{03} \rightarrow 4_{32}(40\ \mu)$, $3_{03} \rightarrow 3_{30}(67\ \mu)$, and $3_{21} \rightarrow 4_{32}(59\ \mu)$.

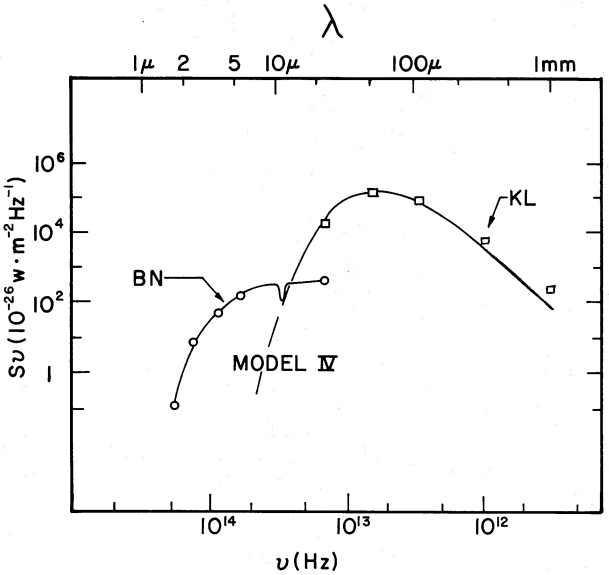

FIG. 5.—Infrared spectra of the Kleinmann-Low nebula and the Becklin-Neugebauer object as measured in a 1′ beam at $\lambda \geq 20\ \mu$. At $\lambda \leq 20\ \mu$ the flux densities are obtained by integrating high-resolution maps over a 1′ beam, and thus we hope to have omitted low surface brightness emission excited by the H II regions. Data are from Becklin *et al.* (1973), Gillett and Forrest (1973), Werner *et al.* (1975), Harper *et al.* (1972), Gezari *et al.* (1974), Werner *et al.* (1974), Rieke *et al.* (1973). The spectrum (inside a 1′ aperture) from model IV (Table 1) has been plotted over the KL data.

Between $\lambda = 350\ \mu$ and 1 mm it is observed that $S_\nu \propto \nu^{3 \rightarrow 3.4}$. From the dependence of the long-wavelength intensity on the emissivity (cf. § IV*d*), we infer that the spectral index n of the emissivity is probably in the range 1.5 to 2. The derived index does depend somewhat on the optical depth and the density distribution, in the sense that if $\tau_{100\,\mu} > 1$ or if the density is constant with radius the spectrum would tend to be less steep and a larger value of n would be required to account for a given falloff. We will conclude in the following discussion that $\tau_{100\,\mu} \lesssim 1$ and therefore $n = 1.5 \rightarrow 1.8$ longward of 100 μ is consistent with the r^{-1} density distribution. In the model calculations $n = 2$ will actually be used. The emissivity law shortward of 100 μ is essentially a guess. In the calculations we have tried two cases: (1) with a change of the emissivity law from λ^{-2} to λ^{-1} shortward to 100 μ (models I, II, III), and (2) with the change from λ^{-2} to λ^{-1} at 30 μ (model IV). The choice of the break at 30 μ in the second case is influenced by the measurements of Knacke and Thomson (1973). Because shortward of 20 μ the contribution to the observed flux due to KL becomes indistinct from that due to the H II region or the infrared point sources, we shall not, in modeling KL, attach any importance to the emissivity shortward of 20 μ. Indeed, the main question about the dust emissivity we address ourselves to is, What is the spectral index of the emissivity that best represents the KL observations, and does the same law hold from 1 mm to 30 μ?

Based on the discussion in § IV*b*, we expect the opacity at the spectral peak of KL ($\sim 70\ \mu$) to be less than or about unity. A stronger limit on this value can actually be placed, using the observed flux at 1 mm and the estimated emissivity law from the earlier paragraph. With a dust temperature of ~ 70 K, as suggested from the brightness temperature at the peak and the ^{12}CO $J = 1 \rightarrow 0$ antenna temperature, the observed 1 mm flux implies an opacity at 1 mm of 0.02. With an emissivity law of $\nu^{1.5 \rightarrow 1.8}$, the corresponding opacity at 100 μ would be 0.6–1.2. In the first three model calculations, with the break of the emissivity law at 100 μ, $\tau_{100\,\mu}$ is taken to have the values of 0.1, 0.5, and 2.5. In the fourth model, with the break of the emissivity law at 30 μ, $\tau_{100\,\mu}$ is set to be 0.5.

For all models the stellar luminosity and temperature are taken to be $10^5\ L_\odot$ and 3600 K.

b) Comparison between Theory and Observations

The spectral distributions in a 1′ aperture of the four model calculations are presented in Figure 4, with the successive spectra shifted down by a factor of 10 for the display. Comparing these theoretical results with the observed values, we can conclude that both very low (model I) and very high (model III) opacities at 100 μ can be ruled out. Model IV provides the best fit to the observed falloff from 50 μ to 20 μ, and also peaks at about 70 μ. We have plotted the spectral distribution of this model on top of the observed values in Figure 5. It is seen that the calculated spectral distribution compares well with the observed one. At 1 mm, the calculated flux is less than the observed value by a factor of 3. If a $\lambda^{-1.5}$ emissivity law were used, the comparison at 1 mm would be better. With model IV, the dust temperature at 2.10^{17} cm is 68 K (cf. Table 1). To summarize, we infer, in light of the model calculations, that the dust density distribution is $n_d \propto r^{-1}$, the emissivity between 30 μ and 1 mm varies approximately as $\lambda^{-1.5}$, and $\tau_{70\,\mu} \approx 1$. With so many parameters that enter into a model calculation it is probably not surprising that a good fit to the observations can be made. Indeed, Werner *et al.* (1975) show that the observed fluxes compare extremely well with the emission from a 70 K blackbody filling the 1′ beam for which the emissivity equals 1 at 20 μ and falls as λ^{-1} to longer wavelengths. What lends credence to our results is that the calculations are performed on a self-consistent basis and the deduced parameters are not completely arbitrary but are estimated based on the general properties of the radiative transfer in a dust cloud.

c) Relationship between BN and KL Nebula

The spectral distribution shortward of the peak might shed some light on the relationship between the BN object and the KL nebula. The simplest interpretation is that the spectrum is a superposition of two spectra, with BN on the near side of the central cluster. For a decreasing density distribution (r^{-1}), and an emissivity law of model IV, BN need not be far from the center of KL. For example, if BN is situated at a radius of 3.10^{17} cm in front of the center, the line-of-sight opacity at 10 μ is ~ 2.5. Thus the positional coincidence between BN and KL is not surprising if stars are formed mostly within a radius of 3.10^{17} cm. However, if the emissivities at 10 μ and 100 μ are in the ratio λ^{-2}, then BN must be situated almost at the front boundary of the cloud to avoid substantial attenuation.

Another interpretation is that BN is the central source responsible for exciting KL. In this situation the observed spectrum places several conditions on the nature of BN and the emissivity law. We distinguish between two cases: first, that in which the observed plateau at 10 μ is largely due to the attenuated radiation from the central source, and, second, that in which it is due to reradiation from hot dust around the source. In the first case, the total luminosity of KL and the observed 10 μ intensity at BN lead to two conditions:

$$4\pi r_*^2 \sigma T_*^4 = L_* = 10^5\ L_\odot\,,$$

$$S_{10\,\mu} = B_\nu(T_*)\pi r_*^2 \exp(-x_{10\,\mu}) = 260\ \text{f.u.} \quad (10)$$

The upper limit on T_*, assuming optical thinness at 10 μ, is ~ 3000 K. This upper limit is unlikely to be realized, since at 10 μ it is certainly not optically thin, else KL would peak at this wavelength. The lower limit is ~ 600 K, and is set by the observed spectral distribution shortward of 10 μ, which can be fitted by a blackbody curve of ~ 600 K. The corresponding upper limit on the *line-of-sight opacity toward the source* at 10 μ, $x_{10\,\mu}$, is 5.3. With model IV this line-of-sight opacity is 8.3. Because of the uncertainty in extrapolating the emissivity from 20 μ to 10 μ, a value of 5.3 for $x_{10\,\mu}$ is not inconsistent with the model for KL. To summarize, the conditions in this case are that the source has a low effective temperature, ~ 1000 K, and that the emissivities between 2 μ and 20 μ be nearly constant. In the other case, if the observed plateau at 10 μ is due to reradiation from surrounding hot dust, no information about the ultimate source can be obtained. However, in order to produce the plateau, the emissivity between 2 μ and 20 μ must again be nearly constant.

We are particularly grateful to Mike Werner for many stimulating discussions and much encouragement in this work. This is contribution number 209 of the Five College Observatory.

REFERENCES

Becklin, E. E., Neugebauer, G., and Wynn-Williams, C. G. 1973, *Ap. J.* (*Letters*), **182**, L7.
Gezari, D. Y., Joyce, R. R., Righini, G., and Simon, M. 1974, *Ap. J.* (*Letters*), **191**, L33.
Gillett, F. C., and Forrest, W. J. 1973, *Ap. J.*, **179**, 483.
Goldreich, P., and Kwan, J. 1974, *Ap. J.*, **189**, 441.
Harper, D. A., Low, F. J., Rieke, G. H., and Armstrong, K. R. 1972, *Ap. J.* (*Letters*), **177**, L21.

Harvey, P. M., Gatley, I., Werner, M. W., Elias, J. H., Evans, N. J., Zuckerman, B., Morris, G., Sato, T., and Litvak, M. M. 1974, *Ap. J.* (*Letters*), **189**, L87.
Knacke, R. F., and Thomson, R. K. 1973, *Pub. A.S.P.*, **85**, 341.
Kwan, J., and Scoville, N. Z. 1976, *Ap. J.* (submitted).
Kwan, J., and Thuan, T. X. 1974, *Ap. J.*, **194**, 293.
Rieke, G. H., Low, F. J., and Kleinmann, D. E. 1973, *Ap. J.* (*Letters*), **186**, L7.
Righini, G., Simon, M., Joyce, R. R., and Gezari, D. Y. 1975, *Ap. J.* (*Letters*), **195**, L77.
Scoville, N. Z., Solomon, P. M., and Jefferts, K. B. 1974, *Ap. J.* (*Letters*), **187**, L63.
Werner, M. W., Elias, J. H., Gezari, D. Y., and Westbrook, W. E. 1974, *Ap. J.* (*Letters*), **192**, L31.
Werner, M. W., Gatley, I., Harper, D. A., Becklin, E. E., Loewenstein, R. F., Telesco, C. M., and Thronson, H. A. 1976, *Ap. J.*, in press.

J. KWAN: Department of Earth and Space Sciences, State University of New York, Stony Brook, NY 11794

N. SCOVILLE: Department of Physics and Astronomy, University of Massachusetts, Amherst, MA 01002